



P-ISSN: 2349-8528

E-ISSN: 2321-4902

IJCS 2018; 6(6): 1830-1838

© 2018 IJCS

Received: 09-09-2018

Accepted: 13-10-2018

Jules Yoda

¹Laboratory of Molecular Chemistry and Materials (LCMM) / Team of Organic Chemistry and Phytochemistry (ECOP) / University of Ouaga I Pr Joseph KI-ZERBO, 03 BP 7021 Ouagadougou 03, Burkina Faso, West Africa

²Department of Medicine, Traditional Pharmacopees and Pharmacy, Institute for Health Sciences Research, 03 BP 7192 Ouagadougou 03, West Africa, Burkina Faso

Djandé Abdoulaye

Laboratory of Molecular Chemistry and Materials (LCMM) / Team of Organic Chemistry and Phytochemistry (ECOP) / University of Ouaga I Pr Joseph KI-ZERBO, 03 BP 7021 Ouagadougou 03, West Africa, Burkina Faso

Correspondence

Jules Yoda

¹Laboratory of Molecular Chemistry and Materials (LCMM) / Team of Organic Chemistry and Phytochemistry (ECOP) / University of Ouaga I Pr Joseph KI-ZERBO, 03 BP 7021 Ouagadougou 03, Burkina Faso, West Africa

²Department of Medicine, Traditional Pharmacopees and Pharmacy, Institute for Health Sciences Research, 03 BP 7192 Ouagadougou 03, Burkina Faso, West Africa

International Journal of Chemical Studies

Synthesis of new 7-hydroxycoumarin derivatives: Crystal structures and fragmentations processes in ESI-MS

Jules Yoda and Djandé Abdoulaye

Abstract

Novel coumarin derivatives, 7-coumarinyl carboxylates were obtained by acylation of 7-hydroxycoumarin in basic medium. The crystal structure and mass spectra of these coumarin derivatives have been studied. In mass spectrometry, we describe the behavior of these compounds, in the context of correlating fragmentation pathways with electronic charges of atoms. The atomic charges obtained by semi-empirical method AM1, are found to be of good prediction for the fragmentation pathways. X-ray crystallographic analysis confirm the structure of these compounds and the reactivity of the 7-hydroxycoumarin to the acylating reagents.

Keywords: 7-hydroxycoumarin, ESI-MS; X-ray diffraction; electronic charges, fragmentation

1. Introduction

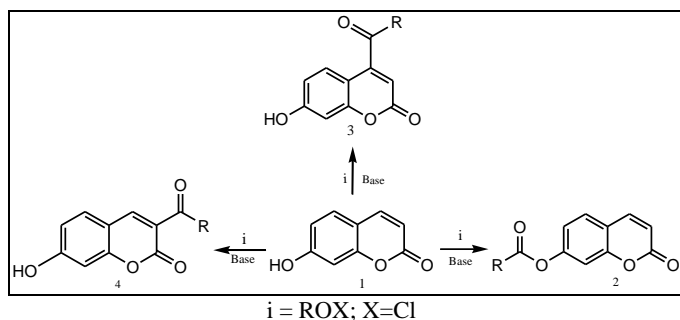
Coumarins are heterocycles prevalent in family of naturally occurring compounds. They are also obtained by synthesis routes. The coumarins and their derivatives are used in the fields of biology, medicine and polymer sciences. They have been identified as anticoagulant [1-3], antibacterial [4], anticancer [5-7], and anti-HIV active [8]. In addition, these compounds are also present or used perfumes and cosmetics [9], alcoholic beverages [10] and laser dyes [11]. As part of the current research on new coumarin derivatives, we study the acylation of 7-hydroxycoumarin. 7-hydroxycoumarin or umbelliferon is the best known compound among hydroxycoumarines. Its derivatives are much studied for their potential pharmacological activity [12-14].

In this study, we analyze the crystal structure and mass spectra (ESI-MS) of a series of 7-hydroxycoumarin derivatives. The ESI-MS analysis has been improved by our research team, by introducing electronic charges in the fragmentation study [15-18]. They showed that the fragmentation of organic compounds, both in electron impact mass spectrometry (EIMS) and electrospray ionization (ESIMS, Positive Mode), is guided by high-charge atoms whose nature is identical to that of the projectile used for ionization. So, for the very first time, we should like to apply the method using electronic charges of atoms in fragmentations study of compounds 2 in ESI/MS. Good results are then obtained. The X-ray diffraction analysis of three compounds further confirms their structure and especially the acylation orientation in basic medium.

2. Materials and Method

2.1 Preparation of 7-coumarinyl carboxylates

The method used for the synthesis of these compounds is based on HSAB theory [18]. This method was developed in our laboratory and used for the preparation of coumarins derivatives [14-16]. In order to understand the reactivity of 7-hydroxycoumarin, the latter is reacted with an acyl chloride or a corresponding acid anhydride in an appropriate solvent in a basic medium as shown in scheme 1. We took into account any acylation products including products 2, 3, 4.



R = aliphatic: solvent = diethylether, base = pyridine
 R = aromatic: solvent = THF; Base = Triethylamine (TEA)

Scheme 1: Acylation of 7-hydroxycoumarin

2.2 Mass Spectra

The analyzes were performed on a 3200 QTRAP (Applied Biosystems SCIEX) mass spectrometer equipped with a pneumatically assisted atmospheric pressure ionization (API) source. The sample was ionized in positive electrospray mode under the following conditions: electrospray voltage (ISV): 5500 V; orifice voltage (OR): 10 V; Nebulization gas pressure (air): 10 psi. The mass spectrum (MS) was obtained with a linear ion trap. The fragmentation spectrum (MS / MS) was obtained after collision induced dissociations (collision gas: N₂, collision energy: 20 eV) in a configuration where the two tandem mass analyzers are quadrupoles. The sample is dissolved in 450 μ l of dichloromethane and then diluted 1/100 in a solution of methanol at 3 mM ammonium acetate. The solution of the extract is introduced into the infusion ionization source (Harvard Apparatus pump-syringe pump) at a flow rate of 10 μ l / min.

2.3 Electronic Charges

The electronic charges were obtained by the Austin Modell semi-empiric method (AM1) [19], using Chem Draw Ultra 8.0

and Chem3D Ultra 8.0 programs from Chem Office 2008 software.

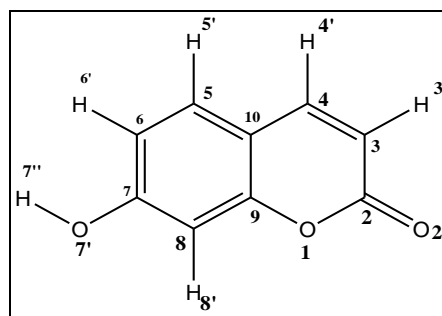
2.4 X-ray Diffraction Analysis

The measurements were performed on a Rigaku Super Nova, Dual, Cu at zero diffractometer equipped with an Atlas S2 detector. Data were collected by the X scan technique at 298 K using CuK α radiation ($\lambda = 1.54184 \text{ \AA}$). The structures were solved by direct methods which revealed the positions of all non-hydrogen atoms, and were refined on F² by a full-matrix least-squares. The program used to solve structure was SIR2014 [20]. The program used to refine the structures was SHELXL2014 [21]. Molecular graphics were generated with Platon [22]. Finally, the software used to prepare material for publications was publCIF [23]. So, in this study, we expose the crystallographic data that justify their 3D structures.

3. Results and Discussion

3.1 Acylation of 7-hydroxycoumarin

In order to have a theoretical approach to the reaction characteristics of 7-hydroxycoumarin, we calculated through the semi-empirical method AM1, the electronic charges of all atoms in compound 1 (Table 1):



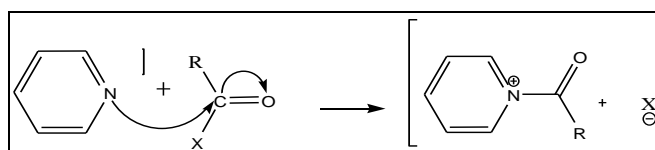
Scheme 2: Structure of compound 1

Table 1: Summary of electronic charges on the structure of compound 1

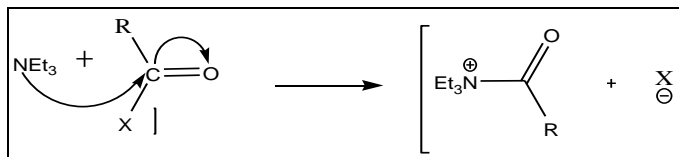
Carbon atoms		Oxygen atoms	
Occupied sites	Electronic charges	Occupied sites	Electronic charge
-	-	1	-0.23691
2	0.38320	2'	-0.31666
3	-0.30974	7'	-0.29611
4	-0.0700	Hydrogen atoms	
5	-0.09247	3'	0.24120
6	-0.23988	4'	0.21312
7	0.12904	5'	0.20699
8	-0.30024	6'	0.22816
9	0.16011	7''	0.26779
10	-0.19923	8'	0.23158

We expect to work according to the method of synthesis with a molar base (pyridine) and a hard base (triethylamine). Since this is an electrophilic substitution, the O-1 sites; C-2; O-2'; C-7; C-9; C-10, will not be affected by the acylation reaction. The C-5, C-4 sites with regard to the absolute value of their electronic charge, the acylation reaction would be less oriented towards these weakly electrophilic sites since the electron density around its sites is relatively low. The sites most likely to react will therefore be: C-6 ($q = -0.2398$), C-8 ($q = -0.3002$); O-7' ($q = -0.29611$); C-3 ($q = -0.3097$). C-acylation can only concern C-3 carbon; C-6 and C-8 having a relatively high negative charge where as O-acylation will only concern oxygen O-7'. The positive charge of the most acidic

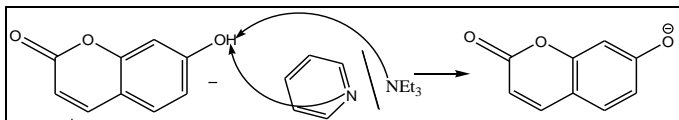
hydrogen H-7'' with a value $q = -0.2677$ exceeds that of the three carbons. The oxygen O-7' should therefore react much faster than the other carbons during an acylation (reaction mechanism diagram 3):



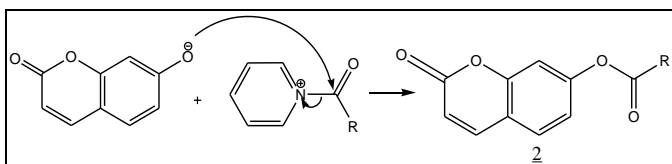
Scheme 3a: First step of the reaction mechanism of the formation of 7-coumarinyl carboxylates (R = alkyl), The reaction between the reagent and the base according to whether R is alkyl or aryl



Scheme 3b: First step of the reaction mechanism of the formation of 7-coumarinyl carboxylates (R = aryle), The reaction between the reagent and the base according to whether R is alkyl or aryl (R = aryle)



Scheme 3c: Second step of the reaction mechanism of the formation of the carboxylates of 7-coumarinyl, the reaction between the substrate and the second mole of the base



2a: R = CH₃; 2b: R = C₂H₅; 2c: R = C₆H₅; 2d: R = *p*-ClC₆H₄; 2e: R = *p*-FC₆H₄; 2f: R = *p*-NO₂C₆H₄; 2g: R = *p*-tBuC₆H₄; 2h: R = *p*-MeC₆H₄; 2i: R = *p*-CH₃OC₆H₄; 2j: R: *p*-CNC₆H₄; 2k: R = *p*-(CH₃)₂NC₆H₄; 2l: 3,5-(NO₂)₂C₆H₃

Scheme 3d: Preparation of 7-coumarinyl carboxylates

3.2 Crystal structure of 7-coumarinyl carboxylate

X-ray diffraction analysis concerned three compounds therefore 2e, 2g and 2h. The single crystals used for diffraction are of prismatic shapes, of colorless yellow and white with varying sizes. The measurements are carried out under the same conditions for all the compounds. A summary of the crystals data, experimental details and refinements results are presented below in the crystal structure determination [24-26].

Regarding the structure of the compounds indicated above, the analysis detects the nature of the constituent atoms of the different molecular skeletons, lengths of the bonds, intra and intermolecule interactions, valence angles, dihedral angles, torsion angles, and so on (figure 1-6). It follows from these analyzes that the molecules in the different single crystals have the following crude formulas: C₁₆H₉FO₄, C₂₀H₁₈O₄, C₁₇H₁₂O₄, which correspond respectively to the compounds 2e, 2g, 2h (figure 1-3). According to the geometry of these different molecular structures, the coumarin nucleus is plane and forms a dihedral angle with the benzene nucleus whose values differ from one structure to another: 2e: 59.03 (15) °; 2g: 60.14 (8) ° and 2h: 33.10 (12) °. The analysis of these crystallographic data obtained confirms O-acylation. The work based on the theoretical calculations is in line with the structures of compounds 2.

3.2.1 Crystal structure determination (2e)

Chemical formula: C₁₆H₉FO₄; Formula weight: 284.23; Crystal description: prism, pale yellow; Melting point (K): 467–468; Crystal system: Monoclinic; space group: P2₁; Temperature (K): 298; Wavelength (Å): λ = 1.54184; Unit cell dimensions: a = 4.0181 (2) Å; b = 5.7296 (3) Å; c = 27.5566 (14) Å; β = 91.660 (4)°; Volume (Å³): 634.14 (6); Z = 2; Radiation type: CuKα; Absorption coefficient (mm⁻¹): 1.00; Density (Mg m⁻³): 1.489; F(000): 292; Crystal size (mm):

0.40 x 0.12 x 0.05; 8239 measured reflections; 2228 independent reflections; R_{int} = 0.026; R[F² > 2σ(F²)] = 0.034; wR (F²) = 0.098; S = 1.13; 2228 reflections; 190 parameters; bond Angles: 111.2 (3) -126.0 (3); torsion Angles 63.4 (4)°; dihedral Angles: 59.03 (15).

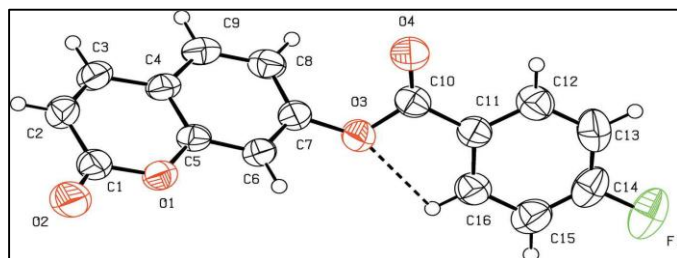


Fig 1: The molecular structure of 2e, along with the atomic numbering scheme. Displacement ellipsoids are drawn at the 50% probability level. H atoms shown as spheres of arbitrary radius. The intramolecular hydrogenbond is indicated by a dashed line

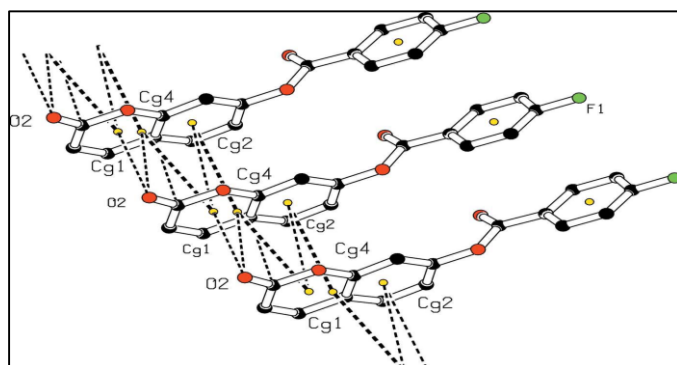


Fig 2: A view of the crystal packing showing C1=O2 and stacking interactions (dashed lines). The yellow dots are ring centroids

3.2.2 Crystal structure Determination (2g)

Chemical formula: C₂₀H₁₈O₄; Formula weight: 322.34; Crystal description: prism, colorless; Melting point (K): 406 - 408; Crystal system: Monoclinic; space group: P2₁/c; Temperature (K): 298; Wavelength (Å): 1.54184; Unit cell dimensions: a = 18.684 (2) Å, b = 6.5431 (5) Å, c = 13.6688(14) Å, β = 93.627(11)°; Volume (Å³): 1667.7 (3); Z = 4; Radiation type: CuKα; Absorption coefficient (mm⁻¹): 0.73; Density (Mg m⁻³): 1.284; F(000): 680; Crystal size (mm): 0.40 × 0.12 × 0.04; 9647 measured reflections; 3005 independent reflections; R_{int} = 0.035; R[F₂ > 2σ(F₂)] = 0.057; wR (F₂) = 0.202; S = 1.01; 3005 reflections; 217 parameters. Bond angles: 111.7 (2) - 124.8(3); torsion Angles: 141.3 (3)°; dihedral Angles: 33.10 (12) °.

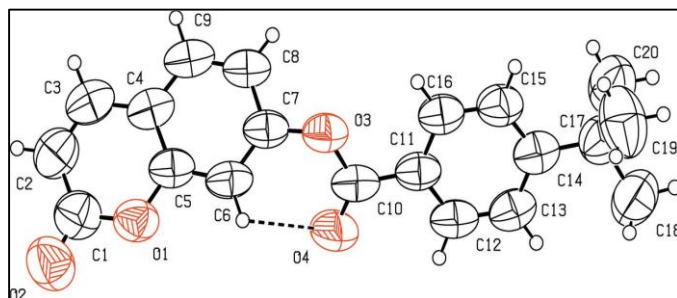


Fig 3: The molecular structure of the title compound and the atomic numbering scheme. Displacement ellipsoids are drawn at the 50% probability level. H atoms are shown as spheres of arbitrary radius. The intramolecular hydrogen bond is indicated by dashed lines

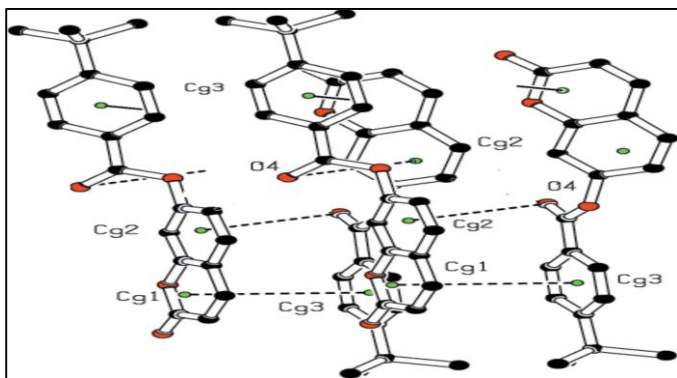


Fig 4: A view of the crystal packing, showing H...H contacts, C10=O4 and stacking interactions (dashed lines). The green dots are ring centroids. H atoms not involved in H...H interactions have been omitted for clarity

3.2.3 Crystal structure Determination (2h)

Chemical formula: $C_{17}H_{12}O_4$; Formula weight: 280.27; Crystal description: prism, pale-yellow; Melting point (K): 435; Crystal system: Monoclinic; space group: Pc; Temperature (K): 298; Wavelength (\AA): $\lambda = 1.54184 \text{\AA}$; Unit cell dimensions: $a = 5.7029(2) \text{\AA}$; $b = 4.0346(1) \text{\AA}$; $c =$

$28.9081(10) \text{\AA}$; $\beta = 90.751(3)^\circ$; Volume (\AA^3): $665.09(4)$ (4); $Z = 2$; Radiation type: CuK α ; Absorption coefficient (mm^{-1}): 0.83; Density (Mg m^{-3}): 1.399; F(000): 292; Crystal size (mm): $0.25 \times 0.16 \times 0.09$; 4661 measured reflections; 1780 independent reflections; $R_{\text{int}} = 0.018$; $R[F_2 > 2\sigma(F_2)] = 0.030$; $wR(F_2) = 0.079$; $S = 1.12$; 1780 reflections; 191 parameters. Bond angles: $116.2(3) - 126.2(4)$; torsion angles: $65.6(4)$; dihedral angles: $60.14(13)^\circ$.

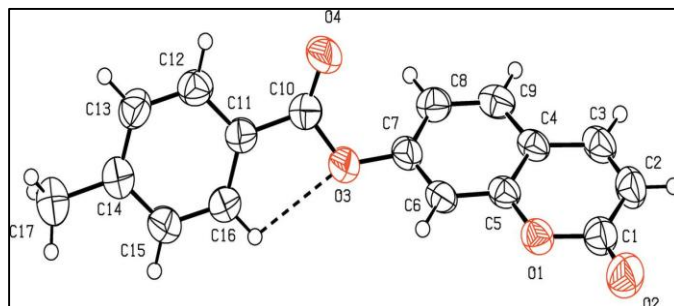


Fig 5: The molecular structure of the title compound with the atomic numbering scheme. Displacement ellipsoids are drawn at the 50% probability level. The dashed line indicates the intramolecular hydrogen bond

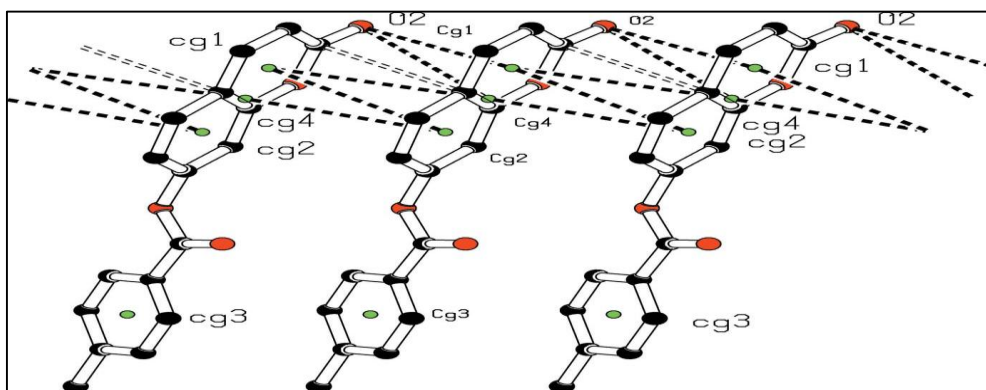


Fig 6: A view of the crystal packing, showing C...C contacts, C1=O2 and stacking interactions (dashed lines). The green dots are ring centroids.

3.3 Analysis of mass spectra

The mass spectrum of the different samples obtained after electrospray positive mode ionization, shows the presence of several signals that can be attributed to the desired compound.

Among these signals, the presence of the pseudo-molecular ion $[M + H]^+$ is observed. This ion was then subjected to a process of fragmentation (MS/MS). The different fragment ions obtained are presented in Table 3.

Table 2a: The fragmentation spectrum of the different pseudo-molecular ions

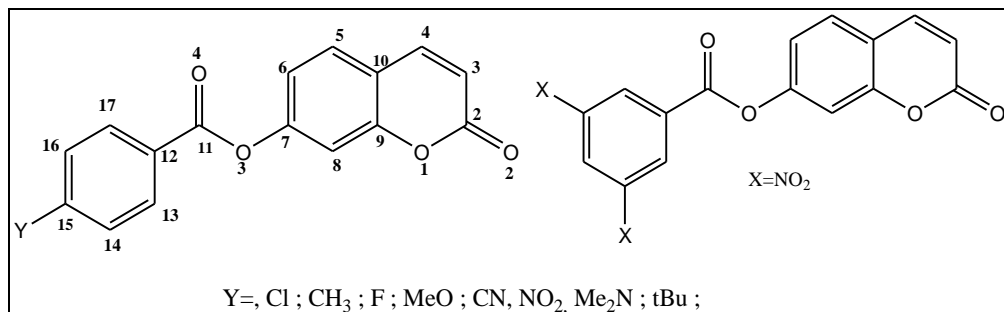
2a R = CH₃		2b R = C₂H₅		2c R = C₆H₅		2d R = <i>p</i>-ClC₆H₄		2^e R = <i>p</i>-FC₆H₄		2f R = <i>p</i>-NO₂C₆H₄	
m/z	%	m/z	%	m/z	%	m/z	%	m/z	%	m/z	%
205 $[M+H]^+$	5	219 $[M+H]^+$	5	267 $[M+H]^+$	14	301/303 $[M+H]^+$	18	285 $[M+H]^+$	3	312 $[M+H]^+$	25
163.1	100	163	100	105	100	139/141	100	123	100	266	1
135	1	119	3	95	0.5	129/131	1	113	1	238	1
107	2	107	2	77	2	113/111	1	95	1	151	2
119	3	99	1	-	-	-	-	-	-	150	100
91	1	-	-	-	-	-	-	-	-	134	2
-	-	-	-	-	-	-	-	-	-	120	17
-	-	-	-	-	-	-	-	-	-	104	6
-	-	-	-	-	-	-	-	-	-	92	10

Table 2b: The fragmentation spectrum of the different pseudo-molecular ions

2g R = <i>p</i>-CH₃C₆H₄		2h R = <i>p</i>-tBuC₆H₄		2i R = <i>p</i>-MeOC₆H₅		2j R = <i>p</i>-CNC₆H₄		2k R = <i>p</i>-Me₂NC₆H₄		2l R = 3,5-(NO₂)C₆H₄	
m/z	%	m/z	%	m/z	%	m/z	%	m/z	%	m/z	%
281 $[M+H]^+$	6	323 $[M+H]^+$	5	297 $[M+H]^+$	4	292 $[M+H]^+$	12	310 $[M+H]^+$	6	357 $[M+H]^+$	100
119	100	161	100	135	100	130	100	148	100	343	2
109	1	146	5	125	1	120	2	134	2	311	31
91	2	133	1	107	1	102	2	120	1	283	4
-	-	118	1	-	-	-	-	-	-	265	34

		105	1						250	2
-	-	91	1	-	-			-	237	9
-	-	-	-	-	-			-	195	87
-	-	-	-	-	-			-	181	4
-	-	-	-	-	-			-	166	5
-	-	-	-	-	-			-	162	5
-	-	-	-	-	-			-	149	19

3.3.1 Electronic charges



Scheme 4: Structure of compounds 2

Table 3a: Electronic charges of atoms of compounds 2

Comp.	C-2	C-3	C-4	C-5	C-6	C-7	C-8	C-9
2a	0,3817	-0,3012	-0,0786	-0,1090	-0,2287	0,11622	-0,2109	0,1280
2b	0,3822	-0,3038	-0,0761	-0,1046	-0,2551	0,1290	-0,2243	0,1332
2c	0,3819	-0,3017	-0,0783	-0,1097	-0,2261	0,1189	-0,2114	0,1277
2d	0,3822	-0,3027	-0,0765	-0,1047	-0,2522	0,1298	-0,2242	0,1338
2e	0,3816	-0,3003	-0,0792	-0,1097	-0,2248	0,1163	-0,2096	-0,1276
2f	0,3810	-0,2965	-0,0816	-0,1091	-0,2232	0,1084	-0,2058	0,1281
2g	0,3818	-0,3021	-0,0781	-0,1098	-0,2261	0,1196	-0,2113	0,1275
2h	0,3825	-0,3047	-0,0753	-0,1049	-0,2533	0,1333	-0,2260	0,1335
2i	0,3818	-0,3022	-0,3022	-0,1101	-0,2255	0,1202	-0,2114	0,1274
2j	0,3814	-0,2989	-0,0798	-0,1090	-0,2257	0,1136	-0,2093	0,1285
2k	0,3829	-0,3070	-0,0738	-0,1052	-0,2540	0,1386	-0,2290	0,1333
2l	0,3804	-0,2933	-0,0835	-0,1084	-0,2226	0,1019	-0,2026	0,1289

Table 3b: Electronic charges of atoms of compounds 2

Comp.	C-10	C-11	C-12	C-13	C-14	C-15	C-16	C-17
2a	-0,1732	0,3559	-0,3649	-	-	-	-	-
2b	-0,1818	0,3665	-0,2666	-0,3502	-	-	-	-
2c	-0,1732	0,4122	-0,1391	-0,1229	-0,2105	-0,1551	-0,2090	-0,1286
2d	-0,1804	0,4241	-0,1416	-0,1135	-0,1979	-0,0507	-0,1965	-0,1199
2e	-0,1715	0,4146	-0,1564	-0,0968	-0,2445	0,1279	-0,2428	-0,1023
2f	-0,1675	0,4067	-0,0992	-0,1377	-0,1450	-0,0985	-0,1436	-0,1436
2g	-0,1734	0,4131	-0,1462	-0,1175	-0,2103	-0,0505	-0,2060	-0,1228
2h	-0,1825	0,4247	-0,1464	-0,1198	-0,2060	-0,0302	-0,2032	-0,1256
2i	-0,1735	0,4179	-0,1784	-0,0910	-0,2338	0,1238	-0,2843	-0,0859
2j	-0,1706	0,4097	-0,1169	-0,1297	-0,1676	0,0127	-0,1664	-0,1362
2k	-0,1850	0,4330	-0,2056	-0,0695	-0,2853	0,1750	-0,2837	-0,0757
2l	-0,1645	0,4146	-0,1501	-0,0335	-0,1576	-0,0395	-0,1557	-0,0396

Table 3c: Electronic charges of atoms of compounds 2

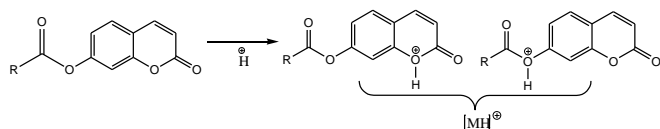
Comp.	O-1	O-2	O-3	O-4	X/ X ₂
2a	-0,2336	-0,3157	-0,2831	-0,3572	-
2b	-0,2342	-0,3167	-0,2860	-0,3603	-
2c	-0,2337	-0,3163	-0,2787	-0,3620	-
2d	-0,2345	-0,3157	-0,2792	-0,3644	Cl:-0,0021
2e	-0,2336	-0,3148	-0,2790	-0,3599	F:-0,1150
2f	-0,2335	-0,3108	-0,2747	-0,3458	N: 0,5173; O: -0,3402; O: -0,3400
2g	-0,2336	0,3168	-0,2793	-0,3634	C:-0,3218
2h	-0,2346	-0,3178	-0,2799	-0,3694	C:-0,0515; C:-0,3372; C:-0,3331; C:-0,3331
2i	-0,2305	-0,3160	-0,2801	-0,3678	C: -0,2101; O:-0,2449
2j	-0,1090	-0,3153	-0,2759	-0,3527	C:-0,0596; N:-0,0695
2k	-0,2349	-0,3203	-0,2834	-0,3803	N:-0,4072; C: -0,1750; C: -0,1752
2k	-0,2327	-0,3073	-0,2717	-0,3368	N: 0,520; N: 0,5292; O:-0,3286; O:-0,3277; O:-0,3290; O:-0,3273

3.3.2 General mode of fragmentation of 7-coumarinyl carboxylate

In the spectra obtained for the majority of the compounds **2**, there is found a reduced number of fragments. The important fragments that we found are those representing the peak-pseudo-molecular $[M + H]^+$, the fragment $R-CO^+$ (acylium ion) and, for the aliphatic groups, the fragment m/z 163. In addition, the fact that the atoms carrying positively high electronic charges is reduced in number. Only carbon atoms C-2; C-7; C-10 and C-11 mean positive electronic charges. Similarly, the number of fragments obtained for each of the components is also proportionally reduced.

3.3.3 Formation of the pseudo-molecular ion $[M+H]^+$

The pseudo-molecular ion, as described below, is obtained after ionization of the molecule M , following the effect of the H^+ projectile. The ionization is certainly done on the oxygen atoms in the state of SP^3 hybridization as oxygen O-1 and O-7 (scheme 2). Indeed p electrons are more mobile than electrons and therefore react more easily with acids. This fragmentation process is generally observed with most of coumarin derivatives [14, 16].



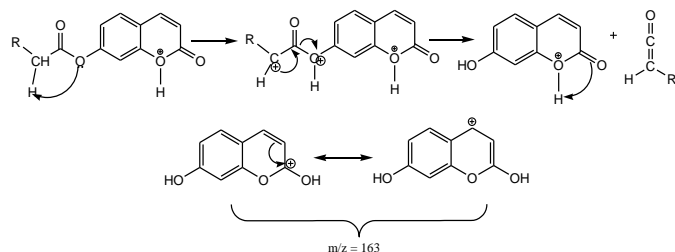
Forme A Forme B

2a: $R = CH_3$ (m/z 205); 2b: $R = C_2H_5$ (m/z 219); 2c: $R = C_6H_5$ (m/z 267); 2d: $R = p-ClC_6H_4$ (m/z 301/303); 2e: $R = p-FC_6H_4$ (m/z 285); 2f: $R = p-NO_2C_6H_4$ (m/z 312); 2g: $R = p-MeC_6H_4$ (m/z 281); 2h: $R = p-tBuC_6H_4$ (m/z 323); 2i: $R = p-CH_3OC_6H_4$ (m/z 297); 2j: $R = p-CNC_6H_4$ (m/z 292); 2k: $R = p-(CH_3)_2NC_6H_4$ (m/z 310); 2l: $R = 3,5-NO_2C_6H_3$ (m/z 357)

Scheme 5: Mechanism of pseudo molecular formation

3.3.4 Fragmentation Specific to Compounds 2a and 2b

Formation of fragment m/z 163: Only two compounds, 2a ($R = CH_3$) and 2b ($R = C_2H_5$) give a very stable fragment at m/z 163 (100 % for 2a and 2b). Considering the high positive charges of the C-11 atoms (2a, $q = 0.3559$, 2b, $q = 0.3665$) of the different compounds, we can propose the following mechanism, always from the form A of the pseudo-molecular ion, for the fragmentation of these compounds ($R = H$ and CH_3).

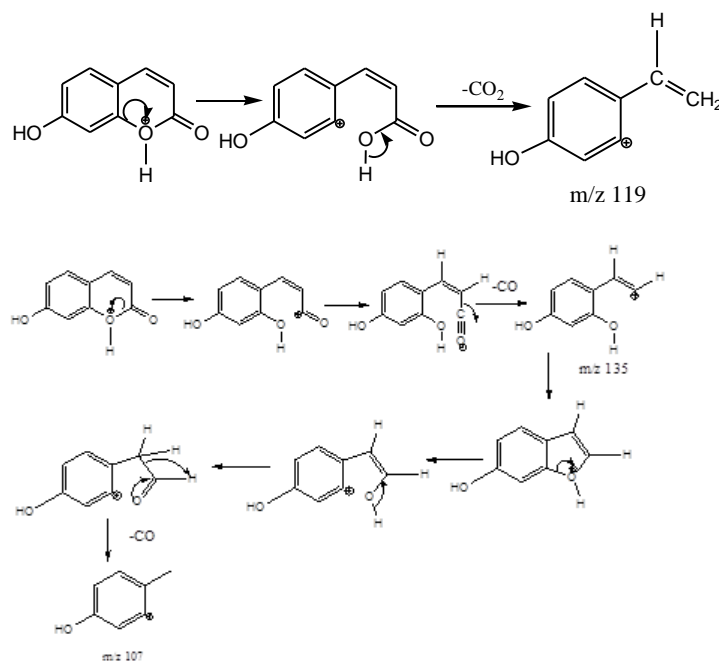


2a: $R' = H$, m/z 163 (100 %); **2b:** $R' = CH_3$ m/z 163 (100 %)

Scheme 6: Fragment/cation formation ($m/z = 163$).

Formation of fragment ions m/z 119 and 107: The fragmentation leading to the unstable ion m/z 119 (3%) occurs at the C-2 carbon site (2a, $q = 0.3822$, 2b, $q = 0.3665$). Compound 2g also gives a fragment at $m/z = 119$. This cation differs from the others in terms of structure and fragmentation mode. We will return to the formation of this fragment ion with the acylium ions. The formation of the m/z 107 ion (2%), as the preceding cation occurs, follows the successive

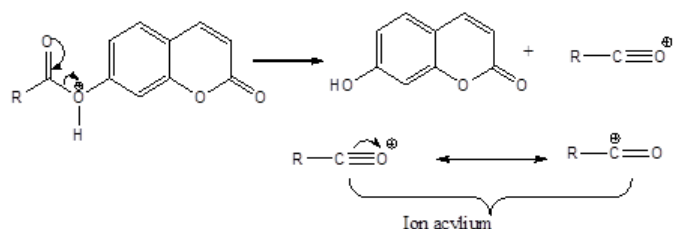
loss of a carbon monoxide neutral moiety (CO) triggered at carbon C-2. This fragmentation passes through an intermediate cation m/z 135 which is also unstable and even absent in the spectrum of compound 2b.



Scheme 7: Formation of fragment ions m/z 107; m/z 119; m/z 135.

3.3.5 Formation of the Acylium ion $R-CO^+$

All the compounds subjected to this spectrometry gave rise to an acylium ion, except the compounds with $R =$ alkyl ($R = CH_3; C_2H_5$). This cation is found in the mass spectra of all hydroxycoumarin esters [15-17]. The process of this fragmentation is oriented by C-11 carbon. This has the high positive electron charge in all molecules. These results are in agreement with those found in the literature [15].



2c: $R = C_6H_5$ (m/z 105); 2d: $R = p-ClC_6H_4$ (m/z 139/141); 2e: $R = p-FC_6H_4$ (m/z 123); 2f: $R = p-NO_2C_6H_4$ (m/z 150); 2g: $R = p-CH_3C_6H_4$ (m/z 119); 2h: $R = p-tBuC_6H_4$ (m/z 161); 2i: $R = p-CH_3OC_6H_4$ (m/z 135); 2j: $R = p-CNC_6H_4$ (m/z 130); 2k: $R = p-(CH_3)_2NC_6H_4$ (m/z 148); 2l: $R = 3,5-NO_2C_6H_3$ (m/z 195).

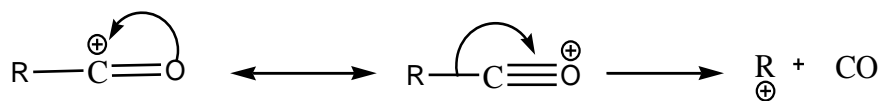
Scheme 8: Formation de lion acylium

3.3.6 Loss of the carbonyl (CO) group from the acylium ion

The loss of the carbonyl group from the acylium ion occurs in almost all cations except the nitro derivatives 2f: $R = p-NO_2C_6H_4$; and 2l: $R = 3,5-NO_2C_6H_3$ (Scheme 9). These compounds are elsewhere and the only ones to produce fragments in large numbers. 9 fragments for 2f and 12 fragments for 2l. This singularity is probably related to the nitro group (NO_2) which is involved in the orientation of the fragmentations with the nitrogen atom (N) the most positively charged $q = 0.5292$, that is why we observe a growth of number of fragments when 2 nitro groups are changed to 2l (table 3). These fragments, for the most part, possess two to

three charges, the multiplicity of which would be bound to the presence of the nitrogen atom in the acylium ion moiety. The dicationic fragments have been observed for diammonium compounds [27]. The authors indicate that their existence is related to the distance separating the two charges. In the

present case these charges are in the para position each other, thus occupying the most distant positions possible in the fragments. The dicationic fragment was observed with the 3-hydroxycoumin esters [16].



2c: R = C₆H₅ (m/z 77); 2d: R = *p*-ClC₆H₄ (m/z 111/113); 2e: R = *p*-FC₆H₄ (m/z 95); 2f: R = *p*-NO₂C₆H₄; 2g: R = *p*-CH₃C₆H₄ (m/z 91); 2h: R = *p*-tBuC₆H₄ (m/z 133); 2i: R = *p*-CH₃OC₆H₄ (m/z 107); 2j: R = *p*-CNC₆H₄ (m/z 102); 2k: R = *p*-(CH₃)₂NC₆H₄ (m/z 120).

Scheme 9: Cation R⁺ formation

3.3.7 Fragments from compound 2f and 2l

As explained above, the fragmentation of compounds **2f**: R = *p*-NO₂C₆H₄ and **2l**: R = 3,5-NO₂C₆H₃ is related to the

electronic contribution of the nitrogen atom. The nitrogen in the structure of the two compounds has the highest positive electron charge (table 4; Scheme 10-11).

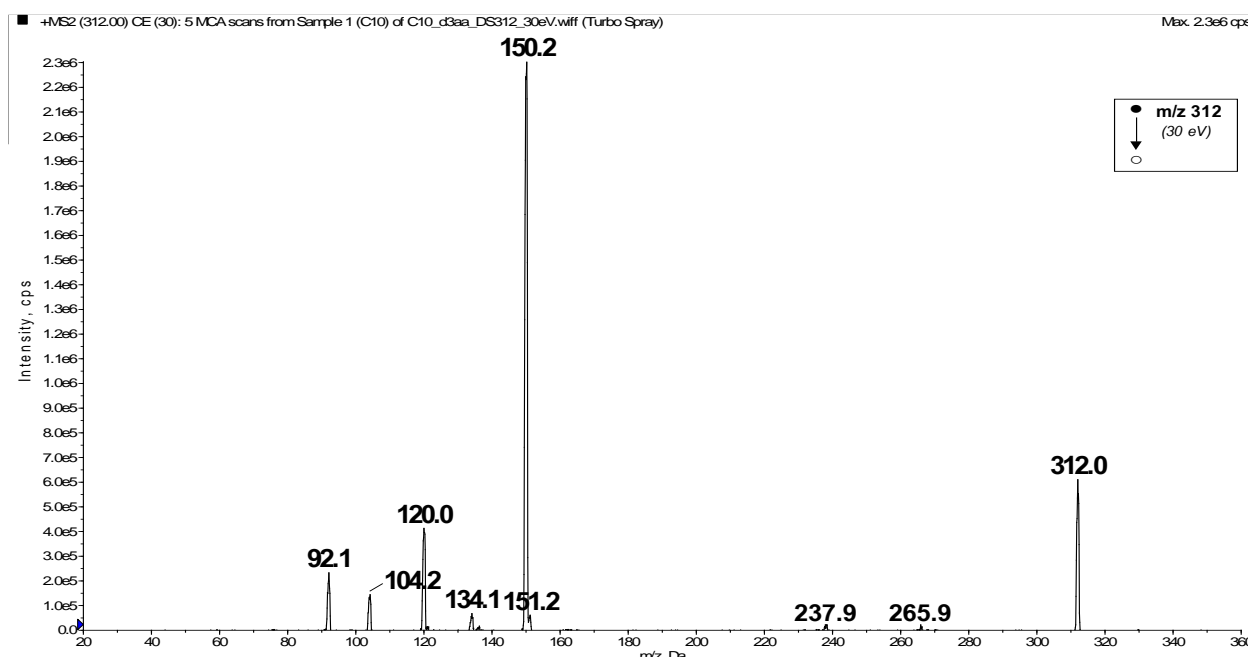


Fig 7: Mass Spectrum of compound 2f

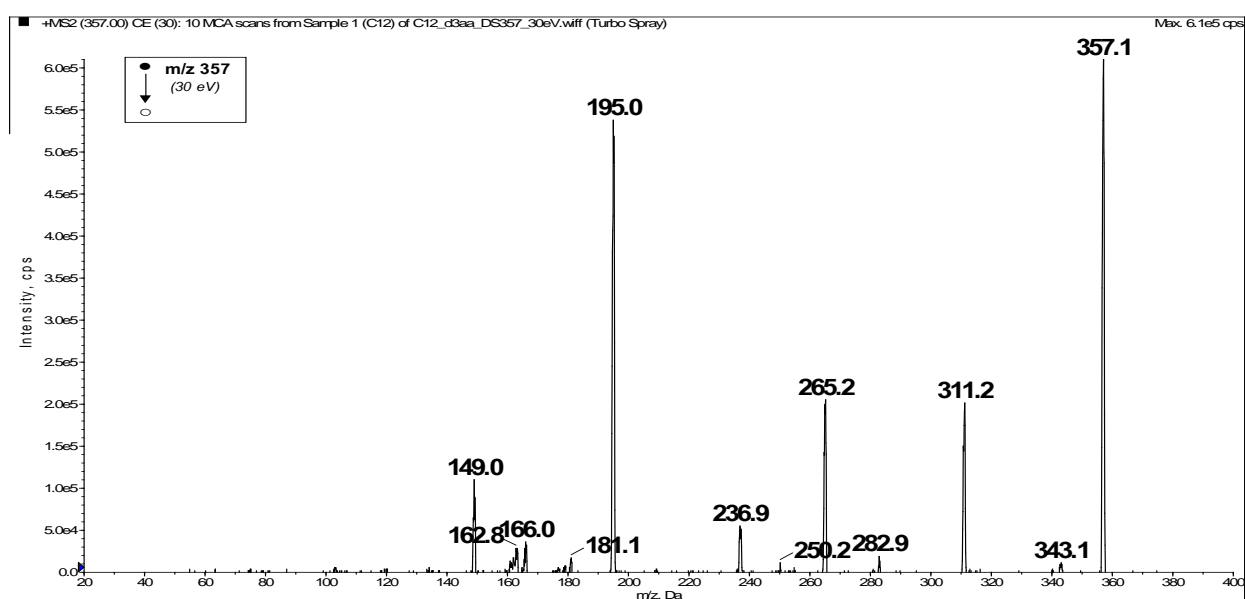
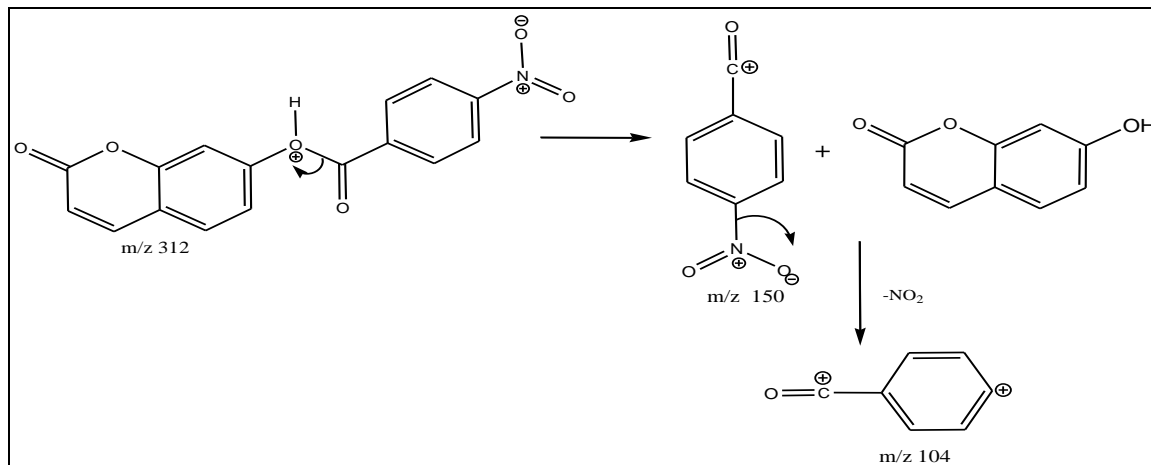
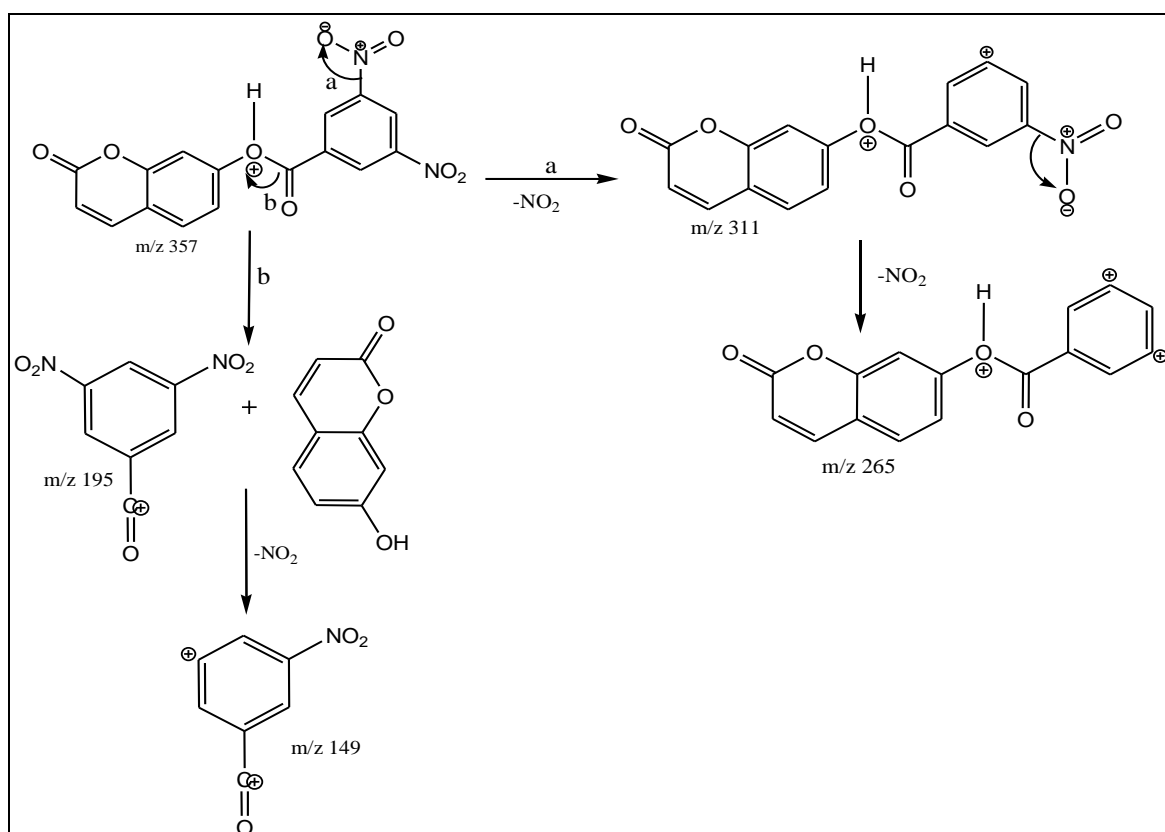


Fig 8: Mass Spectrum of compound 2l



Scheme 10: Formation of fragment ion m/z 104 (6 %); m/z 150 (100 %).



Scheme 11: Formation of fragment ions m/z 311 (31%); m/z 195 (34 %), m/z 149 (87 %); m/z 265 (19 %)

4. Conclusion

This study is part of the research on coumarin heterocycles, aims to expose the results on the acylation reaction of 7-hydroxy coumarins, from aliphatic and aryl acylating agents. Thus analysis of the data makes it possible to confirm the reactivity of the substrate. Theoretical work based on chemical quantum calculations confirms the observed structure.

X-ray diffraction analyzes confirmed the structure of compounds 2 in agreement with results of the theoretical studies. This comes as additional evidence to corroborate the results obtained on the structure of the compounds 2.

The study of 7-coumarinyl carboxylates in mass spectrometry provided us with some interesting information on both the structure and correlation with AM1. It emerges from these studies that in ESI-MS there is a correlation between fragmentation and the value of electronic charges. All

fragmentations take place at atoms carrying positive electronic charges. Some fragments such as the acylium ion typical of hydroxycoumarin esters.

5. References

1. Murray RD. Coumarins. Nat. Prod. Rep. 1989; 6:551.
2. Goodman LS, Gilman A. The pharmacological basis of therapeutics. 5th Ed., MacMillan, New York, 1975.
3. Au N, Rettie AE. Pharmacogenomics of 4-hydroxycoumarin anticoagulants. Drug Metab. Rev. 2008; 40(2):355-375.
4. Bruneton J. Pharmacognosie: Phytochimie, Plantes médicinales. 5th Ed., Tec & Doc, Lavoisier, Paris, 1999.
5. Finn GJ, Creaven BS, Egan DA. A study of the role of cell cycle events mediating the action of coumarin derivatives in human malignant melanoma cells. Cancer Lett. 2004; 214:43-54G.

6. Tusher VG, Tibshirani R, Chu G. Significance analysis of microarrays applied to the ionizing radiation response. *Proc. Nat. Acad. Sci., U S A.* 2001; 98(9):5116-21.
7. Dong Y, Nakagawa-Goto K, Lai C, Morris-Natschke S, Bastow K, Lee K. Antitumor agents 278. 4-Amino-2H-benzo[h]chromen-2-one (abo) analogs as potent *in vitro* anticancer agents. *Bioorg. Med. Chem. Lett.* 2010; 20:4085-4087.
8. Huang L, Yuan X, Yu D, Lee K, Ho Chen C. Mechanism of action and resistant profile of anti-HIV-1 coumarin derivatives. *Virology.* 2005; 332:623-628.
9. O'Kennedy R, Thornes RD. Coumarins: Biology, Applications and Mode of Action, Eds., John Wiley and Sons: Chichester, UK, 1997.
10. Izquierdo MEH, Granados JQ, Mir VM, Martinez MCL. Comparison of methods for determining Coumarins in distilled beverages. *Food chem.* 2000; 70:251-258.
11. Maeda M, Laser Dyes, Aca-demic Press, New York, 1984, 161-167,
12. Joseph KS, Moser AC, Basiaga SBG, Schiel JE, Hage DS. Evaluation of alternatives to warfarin as probes for Sudlow site I of human serum albumin. *J Chromatogr.* 2009; 1216(16):3492-3500.
13. Finn GJ, Kenealy E, Creaven BS, Egan DA. *In vitro* cytotoxic potential and mechanism of action of selected coumarins, using human renal cell lines. *Cancer Lett.*, 2002; 183(1):61-8
14. Song A, Wang X, Lam KS. A convenient synthesis of coumarin-3-carboxylic acids via Knoevenagel condensation of Meldrum's acid with ortho-hydroxyaryl aldehydes or ketones. *Tetrahedron letters*, 2003; 44(9):1755-1758.
15. Yoda J, Chiavassa T, Saba A. Fragmentations processes of 3-coumarinyl carboxylates in ESI/MS and their correlation with the electronic charges of their atoms, *Res. J Chem. Sci.* 2014; 4(4):12-16.
16. Yoda J, Djandé A, Kaboré L, House P, Traoré H, Saba A. EIMS and AM1 study of the fragmentations of 3-coumarinyl Carboxylates: Interpretation from electronic charges of atoms. *J Soc. Ouest-Afr. Chim.* 2016; 041:51-58.
17. Djandé A, Sessouma B, Cisse L, Kaboré L, Bayo K, Tine A, *et al.* AM1 and ESI/MS study of 4-acyl Isochroman-1, 3-diones: Correlation between Electronic charges of Atoms and fragmentation processes, *Res. J Chem. Sci.* 2011; 1(3):78-86.
18. Pearson RG. *Hard. Soft Acids and Bases.* *J Amer. Chem. Soc.* 1963; 85:3583.
19. Dewar MJ, Zoebish EG, Healy EF, Stewart JP. The development and use of quantum mechanical molecular models. 76. AM1: a new general purpose quantum mechanical molecular model. *J Amer. chem. Soc.* 1985; 107:902.
20. Burla MC, Caliandro R, Carrozzini B, Cascarano GL, Cuocci C, Giacovazzo C, *et al.* Crystal structure determination and refinement via SIR2014. *J Appl. Cryst.* 2015; 48:306-309.
21. Sheldrick GM. SHELXT - Integrated space-group and crystal-structure determination. *Acta Cryst.* 2015; A71:3-8.
22. Spek AL. Structure validation in chemical crystallography. *Acta Cryst.* 2009; D65:148-155.
23. Westrip SP. publCIF: software for editing, validating and formatting crystallographic information file. *J Appl. Cryst.* 2010; 43:920-925.
24. Djandé A, Abou A, Kini BF, Kambo KR, Giorgi M. 2-Oxo-2H-chromen-7-yl 4-methylbenzoate IUCrData 2018; 3:x180927.
25. Abou A, Yoda J, Djande A, Coussan S, Zoueu TJ. Crystal structure of 2-oxo-2H-chromen-7-yl 4-fluorobenzoate. *Acta Cryst.* 2018; E74:761-765.
26. Ouedraogo M, Abou A, Djandé A, Ouaric O, Zoueu JT. 2-Oxo-2H-chromen-7-yl 4-tert-butylbenzoate. *Acta Cryst.* 2018; E74:530-534.
27. Pashynska VA, Kosevich MV, Gomory A, Szilagyi Z, Vékey K, Stepanian SG. Rapid. *Commun Mass Spectrom.*, on the stability of the organic dication of the bisquaternary ammonium salt decamethoxinum under liquid secondary ion mass spectrometry. 2005; 19(6):785-97.